Surf-Riding in Multi-Chromatic Seas: "High-Runs" and the Role of Instantaneous Celerity

Nikos Themelis, *School of Naval Architecture and Marine Engineering, National Technical University of Athens*, nthemelis@naval.ntua.gr

Kostas J. Spyrou, *School of Naval Architecture and Marine Engineering, National Technical University of Athens*, k.spyrou@central.ntua.gr

Vadim Belenky, *David Taylor Model Basin / NSWCCD, Maryland, USA*, vadim.belenky@navy.mil

ABSTRACT

We investigate "high-run" events of ships in following seas. These are cases of ship motion when, due to waves' effect, a ship attains abnormally high speed. Investigations are carried out in three directions: firstly, the statistics of high-runs are calculated, exploring in particular their dependence on the wave spectrum and the sea state. Secondly, a rather neglected up to now method, proposed by Grim, for the quantification of the probability of high-run occurrence is implemented. Lastly, the focus is set on the connection of the instantaneous wave celerity with the mean surge velocity during high-run. For its evaluation, two different error metrics are implemented.

Keywords: *ship surging, surf-riding, high-run*

1. INTRODUCTION

A direct approach for calculating the probability of surf-riding of a ship operating in extreme irregular waves could be based on the identification of time intervals in which her speed is maintained at a level that is consistently above the normally expected range. Any individual realisation of such behaviour will be called hereafter "a high run" and it could be considered as generalisation of surf-riding for a multi-frequency wave environment. Whilst its inception requires careful consideration of system's phase-space, empirically it could be recognised by the up-crossing of an appropriate surge velocity threshold such as the instantaneous wave celerity. It is noted however that, for irregular seas, the role of wave celerity for surf-riding capture is still inferred from phenomenology rather than from proof (for some insights see Spyrou et al 2014a). A high-run's end could be similarly defined by the down-crossing of a suitable threshold, which however it is not easy to be uniquely defined through experience.

The literature in the topic is scarce. However, in a pioneering (but rather oversighted) work, Grim had attempted to determine how a ship could be accelerated by waves and then maintain a speed higher than her mean speed, for extended time intervals in irregular seas (Grim 1963). He had called such phenomena "long-runs". By a string of

eloquent and yet quite severe analytical approximations, he had produced statistical estimates of their existence (based on up-crossing of a speed level that he had considered as critical) and their duration.

In the current study the aim was the systematic examination of the probabilistic properties of the high-runs. It is well-known that, the longer a ship maintains a speed higher than normal, the more likely it is to experience the broaching-to instability (Spyrou 1995). The importance of the topic is thus prevalent. Firstly, a campaign of numerical simulations with direct counting of high-run durations was performed. Targeted quantities were: the mean duration of high-run; and the mean time between successive high-runs. Then, the key elements of Grim's approach were implemented, taking advantage however of current numerical calculation capability. Thus, alternative probability figures were derived which could be contrasted against those obtained by direct counting. Our final goal was to examine the correlation of instantaneous wave celerity with surge velocity during high-run incidents.

2. HIGH-RUN STATISTICS

2.1 Mathematical model

The mathematical model of surge motion in following seas was written for an earth-fixed observer, as follows:

$$(m - X_{\ddot{u}})\ddot{\xi} - (\tilde{\tau}_2 \dot{\xi}^2 + \tilde{\tau}_1 n \dot{\xi} + \tilde{\tau}_0 n^2) + (r_1 \dot{\xi} + r_2 \dot{\xi}^2 +$$

$$+ r_3 \dot{\xi}^3) - \sum_{i=1}^{N} Fx_i \sin(k_i \xi - \omega_i t + \varepsilon_i + \varepsilon_{fi}) = 0$$

(1)

where ξ is the longitudinal position of the ship and m, $X_{\ddot{u}}$ are her mass and "surge added mass" respectively. In the summation term denoting wave force, k_i, ω_i and ε_i stand respectively for the i harmonic's wave number,

frequency and random phase. Fx_i denotes the amplitude and ε_{fi} the phase of the harmonic wave force component. Also, n is the propeller rate and r_i, $\tilde{\tau}_i$ are polynomial coefficients appearing in the resistance and thrust force expressions, respectively.

2.2 "High-run" definition

An apparent choice of a velocity threshold whose upcrossing would signal a high-run is the instantaneous wave celerity. Yet, it is known that attraction towards surf-riding is very likely to have started from a slightly earlier time (and thus from a lower velocity). If this early stage is neglected, a small underestimation of the probability should be expected. As down-crossing threshold was set, at first step, the nominal speed. This threshold should not be crossed by speed fluctuations occurring during surf-riding. The nominal speed is a safe choice from this point of view, although a conservative one, possibly contributing to a slight overestimation of probability. This may be statistically cancelled out, at least partly, with the underestimation linked with the beginning of the high-run. As an extra condition we request the surge velocity to be always higher than the nominal speed in order to exclude, in relatively short wave lengths and mild wave height conditions, cases that qualitatively, should not be counted as high runs. In Figure 1 are shown time segments of high-run in accordance to the presented definition. It is desired to obtain the statistics of the high-run's duration as well as of the time interval between successive events of this kind. The mean duration is obtained by summing up all individual durations and then dividing by the number of events:

$$\overline{t}_{\text{high run}} = \sum_{i=1}^{N} t_{\text{high-run}}^{(i)} \Big/ \sum_{i=1}^{N} i$$

(2)

A similar formula is applied for the mean time between high-runs.
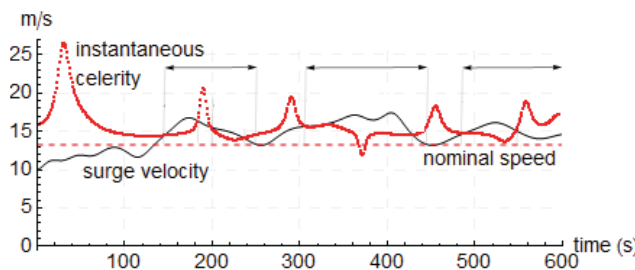
Figure 1   Schematic definition of high-run.

2.3 Simulation settings

The ship selected for applying the calculation schemes is the ONR "tumblehome topside", well-known from several previous studies (for example, Spyrou et al 2014a). A JONSWAP spectrum is considered, discretized by applying a fixed frequency increment $\delta\omega = 2\pi/t_{sim}$ where $t_{sim} = 300\ s$ is the so-called "basis simulation time". The total simulation time was a multiple of it (up to $40 \times t_{sim}$). Four ranges around spectrum's peak were separately examined, assumed containing the wave frequencies participated in the simulations. In Figure 2 are shown the wave amplitudes obtained from the spectrum, considering frequency ranges $0.2\omega_p$ and $0.4\omega_p$. A different choice would have been to modify the wave amplitude so that the variance remains constant. In that case the wave amplitudes obtained would be considerably higher (see again Figure 2). In the current study wave realizations were produced according to the first method, meaning that, the increase of the frequency range increased also the energy.
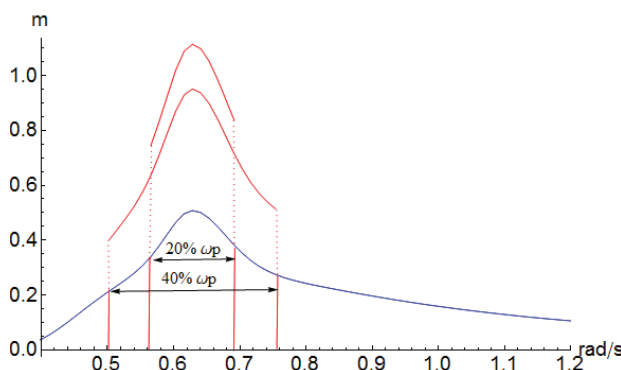
Figure 2   Wave amplitudes for 2 frequency ranges and their modified values when the variance is kept constant. H_S=6 m and T_P=10 s.

Lastly, in Table 1 appear the values of the remaining simulation parameters. Sensitivity studies in relation to the sea state, narrowness of the spectrum and the simulation time were carried out. We run 100 wave realizations per parameters' setting. The nominal and the initial speed of the ship, in each scenario, were not changed (for extra explanations see Spyrou et al 2014b).

2.4 Results

In Figure 3 appear characteristic high-run durations, obtained by simulation. Vast differences are noticed, some high-runs lasting just a few seconds and others reaching 1000 seconds! The probability density function (*pdf*) of the mean duration, based on 100 simulations, is shown in Figure 4. The effect of the sea condition on the mean, and also on certain percentiles, appear in Figures 5 and 6. Convergence with respect to the simulation time is confirmed from Figure 7.

Effect of wave frequency range on mean duration of high-run

When the frequency range is narrow, mean times are higher and they are concentrated around the lower peak periods (Figure 9).

Table 1 Range of the parameters of simulation

Parameter	Value
V_{nom} (m/s) - Fn	12 – 0.308
$V(0)$ (m/s)	10
wave realizations per scenario	100
H_S (m)	(3-6)
T_P (s)	(8.5-13)
(% ω_p one side)	(5-30)
Total simulation time (s)	(t_{sim} - 40xt_{sim})
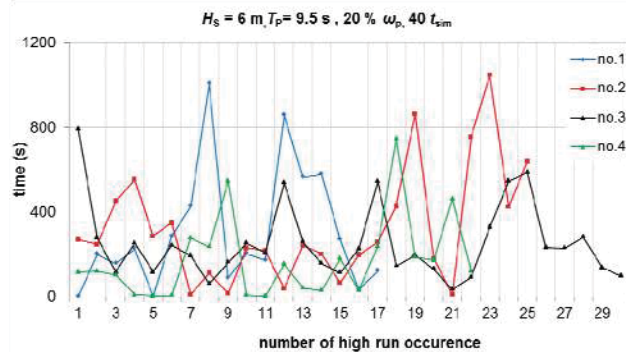
Figure 3 Recorded durations of high-run incidents in different simulations.
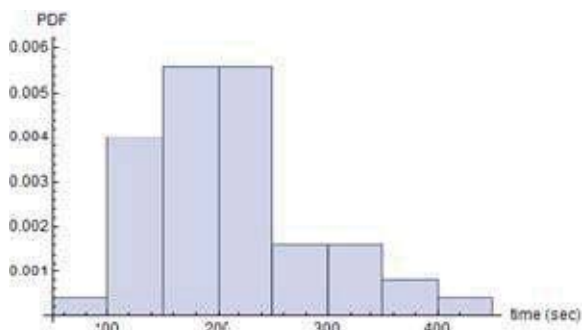
Figure 4 *pdf* of mean high-run duration [H_S=6 m, T_P=9.5 s, 40 t_{sim}, frequencies in 10% ω_P (one side)].

When the range is broadened, so do the peak values of the mean. The trend depends on the assumed significant wave height and it is more pronounced at higher significant wave heights.
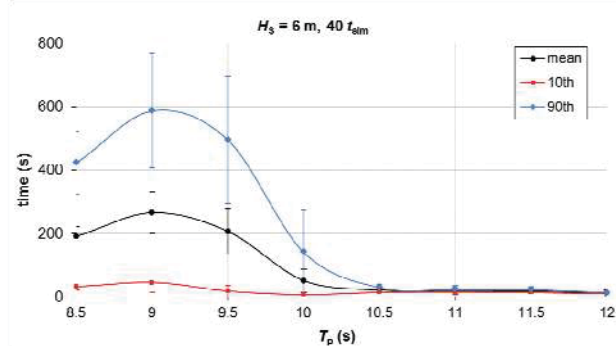
Figure 5 Mean value and percentile means (10th and 90th), as T_P is varied (H_S=6 m and simulation time 40 $t_{sim.}$). Standard deviations are included.
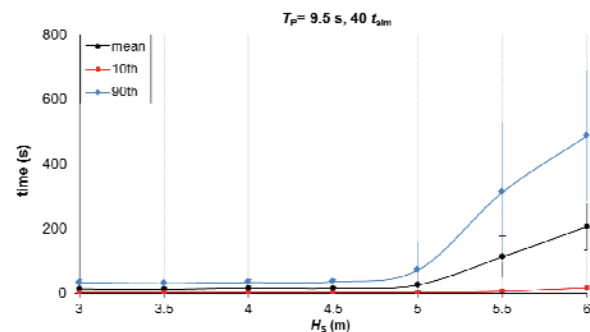
Figure 6 As in Figure 5, with varied significant wave height and fixed peak period.
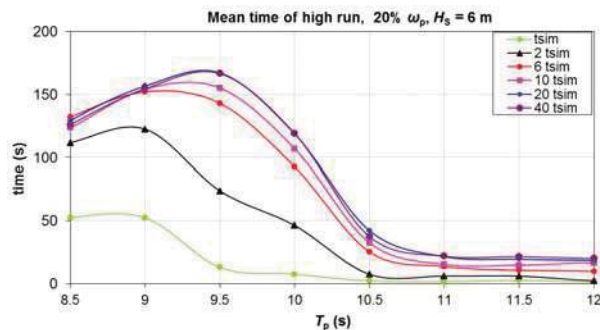
Figure 7 Convergence of statistics.

Effect of wave frequency range on mean time between high-runs

The mean time between successive high-runs is increased with the peak period (Figure 9). The effect of varying the significant wave height can be similarly assessed from Figure 10. The broader the frequency range, the more frequent the high-run occurrence. There seems to be a sharp increase of the mean time beyond a certain value of peak period. On the other

hand, the significant wave height seems more influential when the frequency range is narrow.
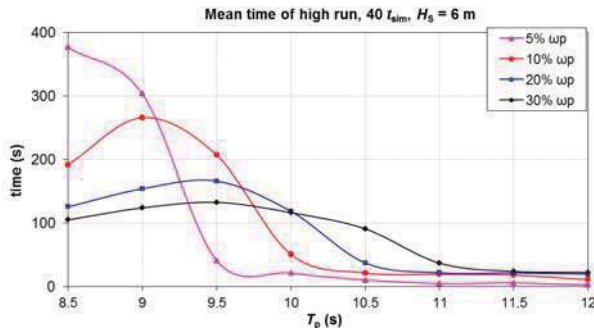
Figure 8 Mean duration of high-run for a gradually broader frequency range, as peak period is varied.
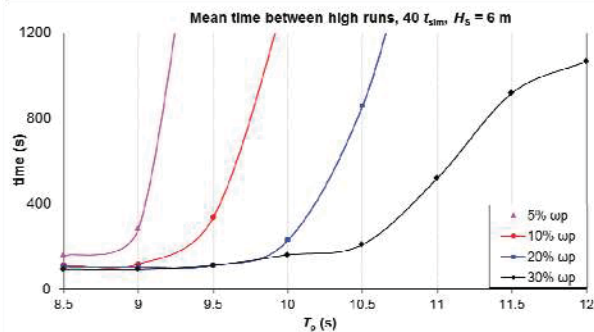
Figure 9 Mean time between successive high-runs as the peak period is varied.
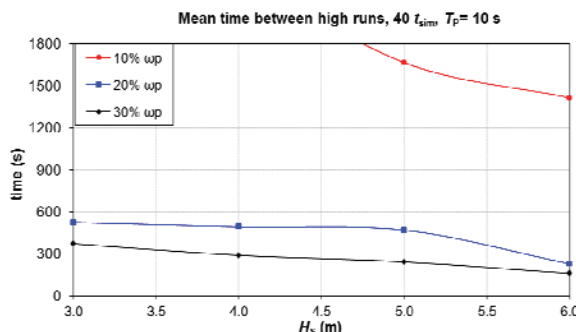
Figure 10 Mean time between high-runs as significant wave height is varied.

3. THE APPROACH OF GRIM

3.1 Key points

The main issue addressed by Grim was the probabilistic quantification of the occurrence and duration of high-run ("long run"), taking into account the strongly nonlinear character of surge motion when the phenomenon occurs, in a following irregular sea (Grim 1963). However, the lack of computer power for the demanding numerical calculations, together with the lack of a theory explaining surf-riding, at that time, had led him to incorporate several simplifying assumptions whose influence was unknown. Grim had focused on the condition generating unusually high surge acceleration and on the duration of the ensuing high speed run, which he assumed represented by a velocity plateau. Thus a simple, trapezoidal structure of ship speed was considered during such incidents. Next is presented a summary of Grim's method.

3.2 Mathematical model set-up

The surge equation is written with respect to an inertial system that moves with the ship's constant nominal speed V. The method assumes that the time is paused at the instant t when high-run's acceleration begins. Later time is measured through a new time variable τ:

$$\ddot{x}_0 + N\left(\dot{x}_0, x_0^2, x_0^3\right)/\left(m - X_{\dot{u}}\right) =$$
$$= \int_0^\infty \cos\left[\frac{\omega^2}{g}x_0 - \omega\left(1 - \frac{\omega \cdot V}{g}\right)(t+\tau) + \varepsilon\right]\sqrt{f_x^2(\omega)S(\omega)d\omega}$$

(3)

The distance variable x_0 determines ship's position. Function $N\left(\dot{x}_0, x_0^2, x_0^3\right)$ refers to the resistance and thrust forces, f_x is the RAO of the Froude-Krylov surge wave force [divided by the mass (including added mass) of the ship] and S is the wave spectrum. Consistently with the model of section 2, the term $N\left(\dot{x}_0, x_0^2, x_0^3\right)$ should take the following form:

$$N\left(\dot{x}_0, x_0^2, x_0^3\right) = \left[3r_3V^2 + 2(r_2 - \tilde{\tau}_2)V + r_1 - \tilde{\tau}_1 n\right]\dot{x}_0 +$$
$$+ \left(3r_3V + r_2 - \tilde{\tau}_2\right)\dot{x}_0^2 + r_3\dot{x}_0^3 + R(V) - T(V;n)$$

(4)

where resistance and thrust, at the nominal speed are, respectively:

$$R(V) = r_1 V + r_2 V^2 + r_3 V^3$$
$$T(V;n) = \tilde{\tau}_2 V^2 + \tilde{\tau}_1 Vn + \tilde{\tau}_0 n^2 \qquad (5)$$

At the critical stage, the ship is assumed under a constant acceleration for a time duration τ_1. When the critical velocity V_{crit} is reached the ship maintains this velocity for time $\tau_2 - \tau_1$ (see eq. 6). Thus, the required acceleration to realise the high run should be: $b = (V_{crit} - V)/\tau_1$.

$$\dot{x}_0 = \begin{cases} b \cdot \tau, & 0 \leq \tau \leq \tau_1 \\ b \cdot \tau_1, & \tau_1 \leq \tau \leq \tau_2 \end{cases} \qquad (6)$$

We note that, whilst for the regular sea he identified celerity as the critical speed, he gave no similar indication for the choice of critical speed in an irregular sea.

The wave force in (3) is considered through its integral for a finite duration τ_1 (impulse function) – this leads to the key idea of producing an impulse spectrum. Integration of (3) in time leads to an equation based on momentum:

$$\int_0^{\tau_1} \left[\ddot{x}_0 + \frac{N\left(\dot{x}_0, x_0^2, x_0^3\right)}{(m - X_{\ddot{u}})} \right] d\tau = \qquad (7)$$
$$= \int_0^{\tau_1}\int_0^{\infty} \cos\left[\frac{\omega^2}{g} x_0 - \omega\left(1 - \frac{\omega \cdot V}{g}\right)(t + \tau) + \varepsilon \right] \sqrt{f_x^2(\omega) S(\omega)} d\omega d\tau$$

Calculating partly the force integral leads to the following expression of the impulse (for details see Grim 1963):

$$\int_0^{\infty} \cos\left[\omega\left(1 - \frac{\omega V}{g}\right) t + \varepsilon' \right] \sqrt{f_x^2(\omega) T^2\left(I^2 + Y^2\right) S(\omega)} d\omega$$
$$(8)$$

where:

$$T^2\left(I^2 + U^2\right) = \left\| \int_0^{\tau_1} e^{i\left[-\omega\left(1 - \frac{\omega V}{g}\right)\tau + \frac{\omega^2}{g}\frac{b}{2}\tau^2 \right]} d\tau \right\|^2 \qquad (8')$$

The term $f_x^2(\omega) T^2\left(I^2 + Y^2\right) S(\omega)$ is the sought impulse spectrum, while ε' is another, but still random, phase. Since the maximum value of the impulse is of interest, the cosine term is set to 1. The impulse is a random

function and Grim assumed that its amplitude follows the Rayleigh distribution. In analogy to the mean wave amplitude, the mean impulse amplitude (or some other percentile average of it) is obtained from the square root of the area under the impulse spectrum, for ω from 0 to ∞.

$$\overline{I}^{(1/n)} = \alpha_{1/n} \sqrt{\int_0^{\infty} f_x^2(\omega) T^2\left(I^2 + Y^2\right) S(\omega)\, d\omega} \quad (9)$$

where the coefficient $\alpha_{1/n}$ obtains specific values depending on the average of the impulse highest $1/n$ amplitudes. For example, $\alpha_{1/10} = 1.8$ corresponds to the average of the $1/10$ highest amplitudes. Additionally, the probability to exceed this average value can be obtained from the Rayleigh density function (3.92%). So, eq. 7 is transformed to the next equation where one can solve for $\alpha_{1/n}$ in order to obtain the probability to reach a critical velocity within time τ_1:

$$b \cdot \tau_1 + \int_0^{\tau_1} \left[N\left(\dot{x}_0, x_0^2, x_0^3\right)/\left(m - X_{\ddot{u}}\right) \right] d\tau = \overline{I}^{(1/n)} \quad (10)$$

By integrating eq. 3 up to $\tau = \tau_2$ and repeating the above procedure, a statistical estimate of the time duration of high-run can be obtained.

3.3 Application and results

The above methodology has been applied through the next steps:

- The critical velocity is set equal to the celerity of spectrum's peak frequency.
- The probability to exceed the targeted velocity in a given time τ_1 is calculated.
- Assuming that the critical velocity has been reached in τ_1, we calculate the probability to exceed certain durations $\tau_2 - \tau_1$ of high runs.
- The procedure is repeated by selecting various critical velocity levels, deriving from the nominal speed.

The nominal speed is 12 m/s and the spectrum is JONSWAP with its full frequency range.

Accelerated motion

In Figures 11 and 12 are shown plots of the calculated probability the ship speed to exceed the defined wave celerity. One could regard the time τ_1 as a fraction of the apparent wave period, i.e. it is comparable to the time, during an encounter wave cycle, when the ship is pushed by the wave. For the selected speed and peak periods, the τ_1 value should be somewhere in the range 18-26s. In Figure 13 several velocity thresholds have been tried. To be noted that the threshold $1.3V_{nom}$ corresponds to the wave celerity of $T_P = 10$ s.

Duration of high-run

The statistics of high-run duration depends on the time τ_1 (see Figure 14). It appears that, the sooner the threshold is reached the longer the high-run will last. However, according to Figure 11, the probability of a velocity threshold crossing becomes significant for $\tau_1 > 20$ s. Given that the threshold has been reached, we examine the effect of peak period and significant wave height on high-run's duration. Thus, Figures 15 and 16, showing the effect of peak period and significant wave height on high-run duration, were drawn for $\tau_1 = 20$ s .
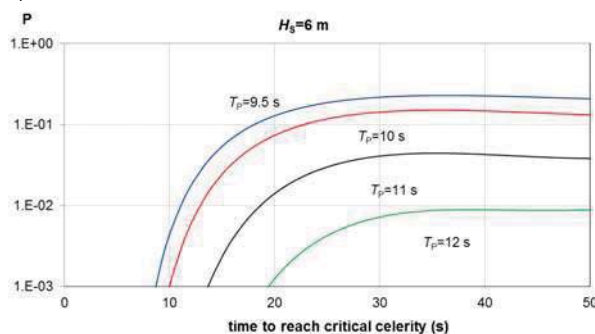
Figure 11 Probability to exceed the celerity value corresponding to the peak frequency, within a certain time, for H_S=6 m.
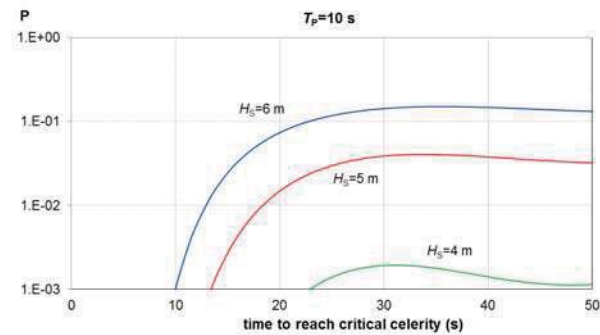
Figure 12 Probability to exceed the celerity value corresponding to the peak frequency, within a certain time, for T_P=10 s.
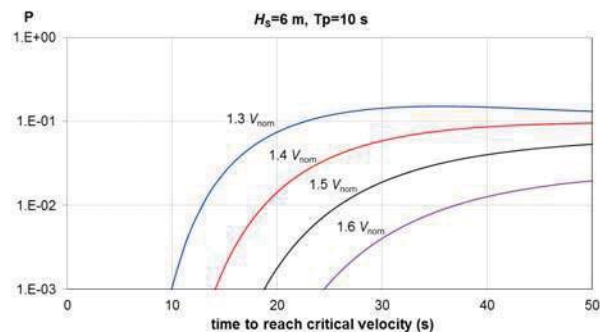
Figure 13 Probability to exceed various values of critical velocity (defined by a constant times the nominal speed) as a function of τ_1 (H_S=6 m and T_P=10 s).

By increasing the peak period, the high-run occur less frequently. One notes in Figure 16 the substantial decrease of the duration for lower significant wave heights. Also, from Figure 17 it is recovered that, setting a higher velocity threshold induces a significant reduction of probability.
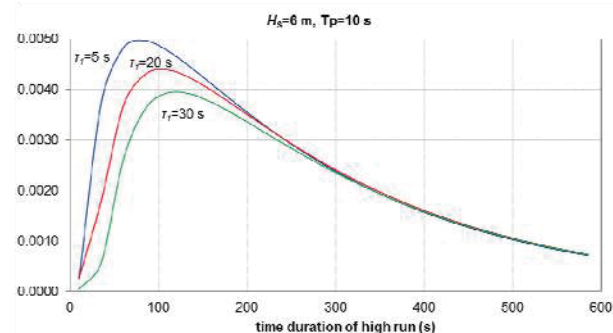
Figure 14 *pdf* of high-run duration for certain wave parameters (3 cases of τ_1).
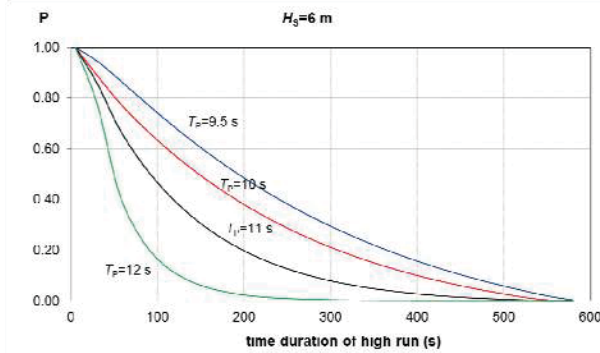
Figure 15 Probability of exceeding a duration value, for several peak periods ($\tau_1 = 20$ s).

3.4 Comparison with direct counting

We contrasted the statistics of high-run duration obtained with the method described in section 2, against the respective result based on Grim's approach (Figure 18). As observed, Grim's method suggests that the longer high-run are more probable (when compared with the mean durations obtained from simulation). This could be also verified by the fact that the mean duration derived from Grim's method (150 s) is approximately equal with the mean obtained for the 80th percentile. A qualitatively similar tendency was noticed also in other sea states.
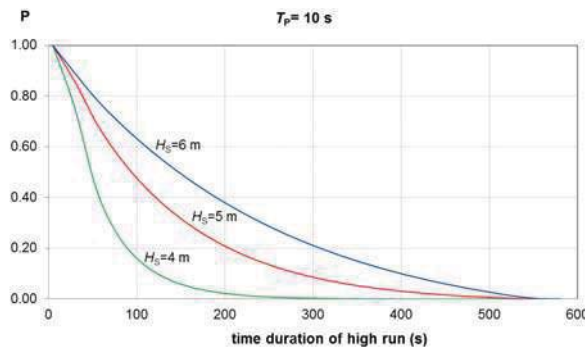
Figure 16 Probability to exceed a duration value. The threshold speed is the celerity corresponding to the peak frequency of the spectrum ($\tau_1 = 20$ s).
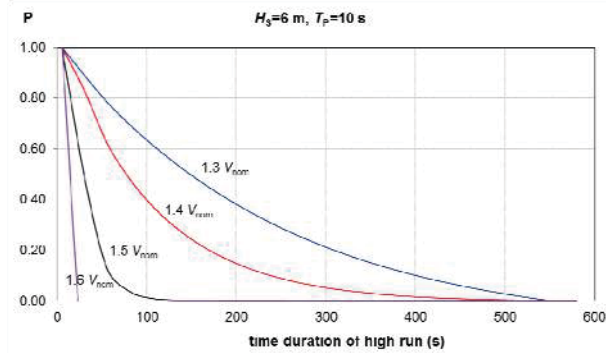
Figure 17 Probability of high-run duration for various velocity thresholds ($\tau_1 = 20$ s).

In interpreting any discrepancies between the results of the two methods, one should take into account their main differences: firstly, Grim's method assumes a constant (and equal to the targeted threshold) surge velocity during the high-run (possibly inspired by the regular wave case when surf-riding occurs). Nonetheless, we have observed fluctuations (sometimes strong) in high-runs. Furthermore, the velocity thresholds that bound the high-run in the two methods are different. In the direct counting, it is specified by the instantaneous wave celerity and the nominal speed while on Grim's approach the limit threshold is constant and equal to the celerity of peak frequency.
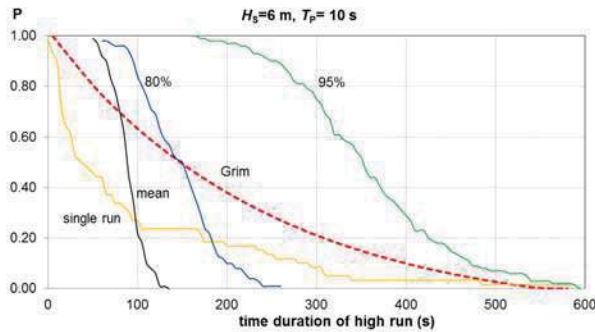
Figure 18 Comparison of probabilities of high-run duration between simulation statistics and Grim's method (H_S=6 m, T_P=10 s).

4. CORRELATION OF CELERITY AND MEAN SPEED IN HIGH-RUNS

4.1 Objectives of the study and error metrics

The aim of this final study is to examine whether could be objectively established that the instantaneous wave celerity truly dictates the mean surge velocity during high-run events. The frequency range is systematically varied in order to study the effect of a transition from a "narrow" to a "broad-band" spectrum. Methods of calculation of the instantaneous wave celerity $c(t)$ in irregular waves were discussed earlier (see Spyrou et al. 2014c). The one used here is derived from the concept of instantaneous frequency.

The mean speed $\bar{U}(t)$ is based on several speed values sampled between successive speed maxima and minima. Details of the calculation procedure are found in Spyrou and Themelis (2013). To quantify the difference between the two time-varying processes of interest (the instantaneous celerity and the mean speed), two error metrics commonly employed in studies addressing discrepancies of time histories will be used (Sarin et. al. 2010). The first metric is the well-known Euclidean vector norm:

$$L_2 = \left\| \mathbf{c} - \bar{\mathbf{U}} \right\| = \left(\sum_{i=1}^{N} \left| c_i - \bar{U}_i \right|^2 \right)^{1/2} \tag{11}$$

where $\mathbf{c}, \mathbf{U}$ are the discretised time histories (vectors of equal dimension N) of instantaneous celerity and mean speed, respectively. It should be noted that vector norms cannot distinguish an error due to phase difference from an error due to magnitude.

The second error metric has been proposed by Sprague and Geers (2004). It combines the error M due to magnitude differences (eq. 12) and the error P due to those of phase (eq.13):

$$M = \sqrt{\frac{\psi_{AA}}{\psi_{BB}}} - 1 \tag{12}$$

$$P = \frac{1}{\pi} \cos^{-1} \left(\frac{\psi_{AB}}{\sqrt{\psi_{AA} \cdot \psi_{BB}}} \right) \tag{13}$$

where

$$\psi_{AA} = \frac{\sum_{i=1}^{N} c_i^2}{N}, \ \psi_{BB} = \frac{\sum_{i=1}^{N} \bar{U}_i^2}{N}, \ \psi_{AB} = \frac{\sum_{i=1}^{N} c_i \bar{U}_i}{N} \tag{14}$$

The combined error is:

$$C_{er} = \sqrt{M^2 + P^2} \tag{15}$$

These two error metrics will be applied not only to the instantaneous celerity versus the mean speed, but also to the celerity corresponding to the peak frequency versus the mean speed, because the latter is also a strong candidate for the critical speed of surf-riding.

4.2 Simulation settings

The "tumblehome" vessel is assumed operating at nominal speed 14 m/s. Ranges of wave frequency with gradually increasing width are tested (JONSWAP spectrum). Per frequency range, 10 realisations are generated. The significant wave height and the peak period are 6 m and 10 s, respectively. The total simulation time is 5000 s; however the first 2000 s of each run are excluded from further processing. The time step is 1 s.

4.3 Results

Error mean values according to the two applied metrics were obtained. To ensure that the comparison is carried out only during time segments of high run occurrence, we introduced a velocity condition requiring, the mean surge velocity to be greater than the nominal speed ($\bar{U}(t) > U_{nom}$) ("1st velocity condition"). We tested also a slightly modified version of it: $\bar{U}(t) > 1.1 \cdot U_{nom}$ ("2nd velocity condition"). Finally, we calculate the error values between the mean of the surge velocity and the mean of the instantaneous celerity. For

the latter, we follow the same calculation procedure as for the mean surge velocity.

Typical time histories on which the two metrics are applied are shown in Figure 19. Errors according to the Euclidean metric are seen in Figure 21 and 22, for the first and the second velocity condition, respectively. In contrast, Figures 23 and 24 show the errors according to the Sprague and Speers metric. The results based on the Euclidean metric suggest that, the discrepancy of mean speed from the celerity of peak frequency is consistently less than that of mean speed from instantaneous celerity. This trend appears too if the 2nd velocity condition ($\bar{U}(t) > 1.1 \cdot U_{nom}$) is imposed. The same conclusion is drawn when the Sprague-Geers metric is used, if the first velocity condition is applied.
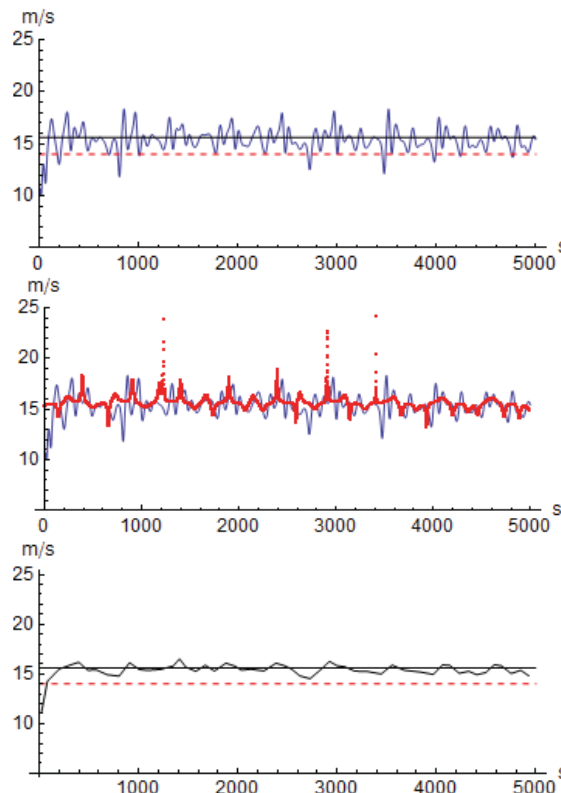
Figure 19 Time histories of surge velocity (upper diagram), instantaneous wave celerity (middle) and mean surge velocity (low). Continuous and dashed straight lines show the wave celerity of the peak frequency and the nominal speed, respectively. The simulations

were based on a frequency range 20% ω_p (both sides).

However, for the second velocity condition the situation is reversed and the correlation of instantaneous celerity with mean speed is superior, for frequency ranges up to 45% ω_p. Even better correlation is achieved when the mean of the instantaneous celerity is taken, in place of the instantaneous celerity itself. In general, the error increases as the frequency range of the spectrum is broadened.

5. CONCLUDING REMARKS

The statistics of high-run occurrences in irregular seas were investigated by simulation–based direct counting and by an approximate semi-analytical method. The topic remains open since the dynamics behind these events is not completely understood yet. The velocity of the high-run shows good correlation with the mean instantaneous celerity when an error metric combining errors of amplitude and phase is applied.
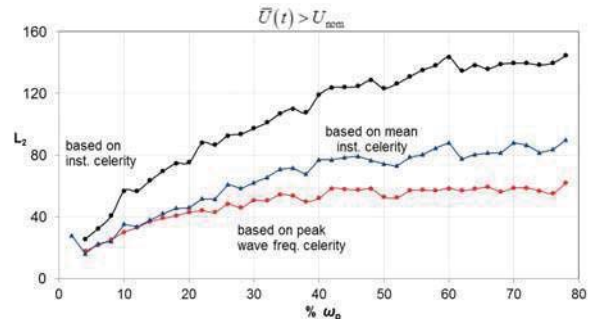
Figure 20 Calculated error according to Euclidean metric (1st velocity condition)
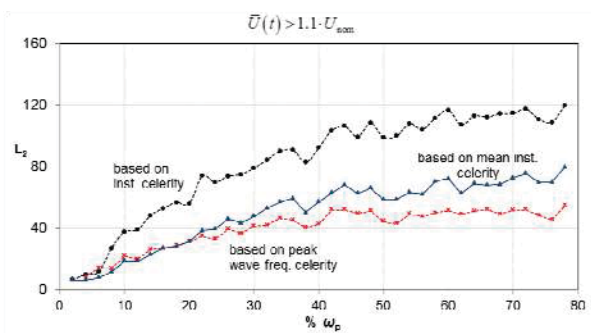
Figure 21 Calculated error according to Euclidean metric (1st velocity condition).
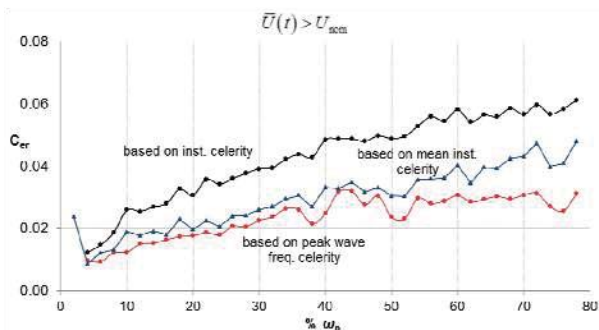
Figure 22 Error according to the Sprague and Geers metric, when satisfying the 1st velocity condition.
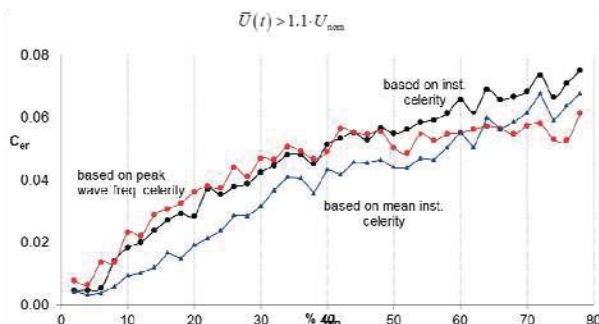
Figure 23 Error according to the Sprague and Geers metric when satisfying the 2nd velocity condition.

6. ACKNOWLEDGEMENTS

7. REFERENCES

Grim, O., 1963, "Surging motion and broaching tendencies in a severe irregular sea", Ocean Dynamics, Vol. 16, No 5, Springer Berlin/Heidelberg, pp. 201-231

Spyrou, K., 1995, Surf-riding, yaw instability and large heeling of ships in following/ quartering waves, Ship Technology Research/Schiffstechnik, 42 (2), 103-112

Spyrou, K., Themelis, N., 2013, "Wave celerity in a multi-chromatic sea: a comparative study", Proceedings, 13th International Ship Stability Workshop, Brest, France.

Spyrou, K., Belenky, V., Themelis, N., Weems, K., 2014a, "Detection of surf-riding behavior of ships in irregular seas", Nonlinear Dynamics, Vol. 78 (1), 649-667, Springer.

Spyrou, K., Themelis, N., Kontolefas, I., 2014b, "What is surf-riding in irregular seas?", Proceedings, 14th International Ship Stability Workshop, Kuala Lumpur, Malaysia, 29th September- 1st October 2014.

Spyrou, K., Belenky, V., Reed,A., Weems,K., Themelis,N., Kontolefas, I., 2014c, "Split-Time Method for Pure Loss of Stability and Broaching-To", Proceedings, 30th Symposium on Naval Hydrodynamics, Hobart, Tasmania, Australia, 2-7 November 2014.

Sarin, H., Kokkolaras, M., Hulbert, G., Papalambros, P., Barbat, S., Yang, R., 2010, "Comparing time histories for validation of simulation models: error measures and metrics", Journal of Dynamic Systems, Measurement, and Control, vol.132.

Sprague, M. A., and Geers, T. L., 2004, "A Spectral-Element Method for Modelling Cavitation in Transient Fluid-Structure Interaction," Int. J. of Numerical Methods Eng., vol. 60, pp. 2467–2499.